Active Species of Horseradish Peroxidase (HRP) and Cytochrome P450: Two Electronic Chameleons

Sam P. de Visser,[†] Sason Shaik,*,[†] Pankaz K. Sharma,[†] Devesh Kumar,[†] and Walter Thiel[‡]

Contribution from the Department of Organic Chemistry and the Lise Meitner-Minerva Center for Computational Quantum Chemistry, The Hebrew University of Jerusalem, 91904 Jerusalem, Israel, and Max-Planck-Institut für Kohlenforschung, Mülheim an der Ruhr, Germany

Received August 24, 2003; E-mail: sason@yfaat.ch.huji.ac.il

Abstract: The active site of HRP Compound I (Cpd I) is modeled using hybrid density functional theory (UB3LYP). The effects of neighboring amino acids and of environmental polarity are included. The low-lying states have porphyrin radical cationic species (Por$^{•+}$). However, since the Por$^{•+}$ species is a very good electron acceptor, other species, which can be either the ligand or side chain amino acid residues, may participate in electron donation to the Por$^{•+}$ moiety, thereby making Cpd I behave like a chemical chameleon. Thus, this behavior that was noted before for Cpd I of P450 is apparently much more wide ranging than initially appreciated. Since chemical chameleonic behavior property was found to be expressed not only in the properties of Cpd I itself, but also in its reactivity, the roots of this phenomenon are generalized. A comparative discussion of Cpd I species follows for the enzymes HRP, CcP, APX, CAT (catalase), and P450.

Introduction

Many oxo-iron heme based enzymes, such as cytochrome P450 (P450), chloroperoxidase (CPO), cytochrome c peroxidase (CcP), catalase (CAT), and horseradish peroxidase (HRP) appear in nature. Among these, P450 is a powerful catalyst for oxygen transfer reactions and is involved in the hydroxylation of alkanes, epoxidation of alkenes, sulfoxidations, etc.[1,2] While the primary function of HRP is as an electron sink,[2e] this enzyme can also perform highly enantioselective transformations in an efficient way.[3] As a result, there is a growing interest in the use of biocatalysts, such as these, for the commercial production of chiral drugs.[3] It is important, therefore, to understand the nature and reactivity of the active species of these types of enzymes. The active species, called Compound I (Cpd I),[4] of the enzyme HRP is fairly long-lived and was one of the first heme-

containing enzymes of which an X-ray structure became available.[5,6] Since then, a lot of research has been devoted to the reactivity and electronic properties of this enzyme. And just recently, all intermediates of the catalytic cycle of HRP were characterized by means of high-resolution X-ray crystallography.[7]

Scheme 1 shows the active sites and some critical amino acids of the proximal pocket of HRP,[7] CcP,[8-10] P450,[11] and CAT[12] with structures taken from the protein data bank.[12] The active species of HRP contains an oxo-iron porphyrin that is linked to the amino acid chain via an imidazole side chain of a histidine residue (His$_{170}$); see Scheme 1. An identical linkage appears in the active species of CcP, the so-called Compound ES (Cpd ES).[8-10] By contrast, P450 uses a thiolate linkage of a cysteine residue.[1,2,11] CAT is another heme-containing enzyme, in which the link is via a phenolate moiety of a tyrosine residue.[13] In both CcP and HRP, the other nitrogen atom of the imidazole

[†] The Hebrew University of Jerusalem.
[‡] Max-Planck-Institut für Kohlenforschung.

(1) (a) Kadish, K. M., Smith, K. M., Guilard, R., Eds. *The Porphyrin Handbook*; Academic Press: San Diego, CA, 2000. (b) Ortiz de Montellano, P. R., Ed. *Cytochrome P450: Structure, Mechanisms and Biochemistry*, 2nd ed.; Plenum Press: New York, 1995. (c) Woggon, W.-D. *Top. Curr. Chem.* **1996**, *184*, 39–95. (d) Meunier, B.; Bernadou, J. *Top. Catal.* **2002**, *21*, 47–55. (e) Woggon, W.-D.; Wagenknecht, H. A.; Claude, C. *J. Inorg. Biochem.* **2001**, *83*, 289–300 (f) Guengerich, F. P. *Chem. Res. Toxicol.* **2001**, *14*, 612–630. (g) Groves, J. T. *J. Chem. Educ.* **1985**, *62*, 928–931.
(2) (a) Sono, M.; Roach, M. P.; Coulter, E. D.; Dawson, J. H. *Chem. Rev.* **1996**, *96*, 2841–2887. (b) Dawson, J. H. *Science* **1988**, *240*, 433–439. (c) Ozaki, S.-i.; Ortiz de Montellano, P. R. *J. Am. Chem. Soc.* **1995**, *117*, 7056–7064. (d) Ortiz de Montellano, P. R. *Annu. Rev. Pharmacol. Toxicol.* **1991**, *32*, 89–107. (e) Poulos, T. L. In *The Porphyrin Handbook*; Kadish, K. M., Smith, K. M. Guilard, R., Eds.; 2000; Volume 4, Chapter 32, pp 189–218.
(3) Adam, W.; Heckel, F.; Saha-Möller, C. R.; Schreier, P. *J. Organomet. Chem.* **2002**, *661*, 17–29.
(4) For general reviews on Compound I species, see: (a) Harris, D. L. *Curr. Opin. Chem. Biol.* **2001**, *5*, 724–735. (b) Harris, D. L.; Loew, G. H. *J. Porphyrins Phthalocyanins* **2001**, *5*, 334–344. (c) Loew, G. H.; Harris, D. L. *Chem. Rev.* **2000**, *100*, 407–419.

(5) Chance, B.; Powers, L.; Ching, Y.; Poulos, T. L.; Schonbaum, G. R.; Yamazaki, I.; Paul, K. G. *Arch. Biochem. Biophys.* **1984**, *235*, 596–611.
(6) Penner-Hahn, J. E.; Smith Eble, K.; McMurry, T. J.; Renner, M.; Balch, A. L.; Groves, J. T.; Dawson, J. H.; Hodgson, K. O. *J. Am. Chem. Soc.* **1986**, *108*, 7819–7825.
(7) Berglund, G. I.; Carlsson, G. H.; Smith, A. T.; Szöke, H.; Henriksen, A.; Hajdu, J. *Nature* **2002**, *417*, 463–468.
(8) Finzel, B. C.; Poulos, T. L.; Kraut, J. *J. Biol. Chem.* **1984**, *259*, 13027–13036.
(9) Chance, M.; Powers, L.; Poulos, T. L.; Chance, B. *Biochemistry* **1986**, *25*, 1266–1270.
(10) Goodin, D. B.; McRee, D. E. *Biochemistry* **1993**, *32*, 3313–3324.
(11) Schlichting, I.; Berendzen, J.; Chu, K.; Stock, A. M.; Maves, S. A.; Benson, D. E.; Sweet, R. M.; Ringe, D.; Petsko, G. A.; Sligar, S. G. *Science* **2000**, *287*, 1615–1622.
(12) Berman, H. M.; Westbrook, J.; Feng, Z.; Gilliland, G.; Bhat, T. N.; Weissig, H.; Shindyalov, I. N.; Bourne, P. E. *Nucleic Acids Res.* **2000**, *28*, 235–242.
(13) Benecky, M. J.; Frew, J. E.; Scowen, N.; Jones, J. P.; Hoffman, B. M. *Biochemistry* **1993**, *32*, 11929–11933.
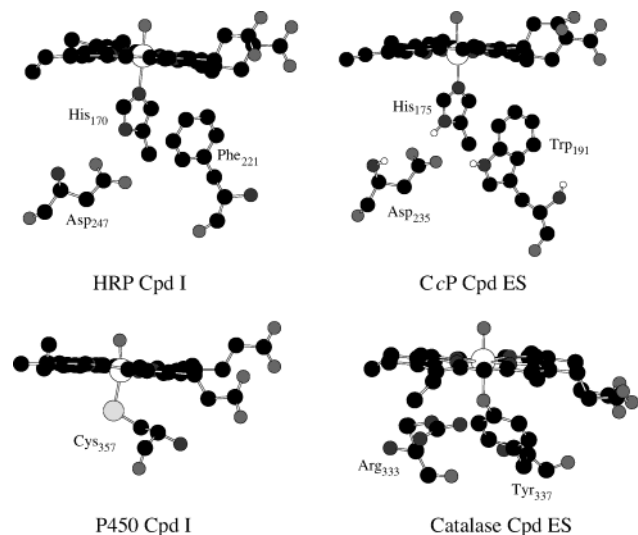
linkage forms a hydrogen bond with a neighboring aspartic acid residue; in the acidic form, the imidazole is protonated. In the case of C*c*P, the carboxylic group of this aspartic acid also forms a hydrogen bond with an indole group of a tryptophan residue (Trp$_{191}$). In HRP, however, this tryptophan amino acid is not available and a phenylalanine amino acid (Phe$_{221}$) takes its place. Although the active sites of all heme-containing enzymes share a great many similarities,[2e,14] their reactivity shows marked differences.[2] Thus, P450 is known to preferentially hydroxylate C−H bonds, while HRP and its mimetic complexes are more prone to act as an electron sink[2e] and to epoxidize double bonds.[15,16] Moreover, HRP oxidizes a variety of small molecules, while C*c*P oxidizes mainly cytochrome *c*, and CPO chlorinates hydrocarbons alongside its P450 and peroxidase activities.[1c,e,2b,e] Obviously, seemingly small differences surrounding the active site change the function of the catalyst, which in all cases reacts via Cpd I. This has prompted us to take on a density functional study of the histidine bound active sites (as in HRP and C*c*P) and compare them with the previously studied[17,18] cysteine bound active sites in P450. In the case of P450, Cpd I was shown to behave like a chameleon species that changes its character due to changes in environmental factors.[4a,17,18] Thus, the addition of two NH- - -S hydrogen bonds to the sulfur atom of the cysteinate ligand, postulated to stabilize the thiolate character,[14] was indeed found to transform the system from a sulfur radical to a porphyrin cation radical; the latter character increases with the increased strength[18] of the hydrogen bonds. The present paper focuses on the active site of an HRP Cpd I model and investigates the environmental effects on the electronic states,
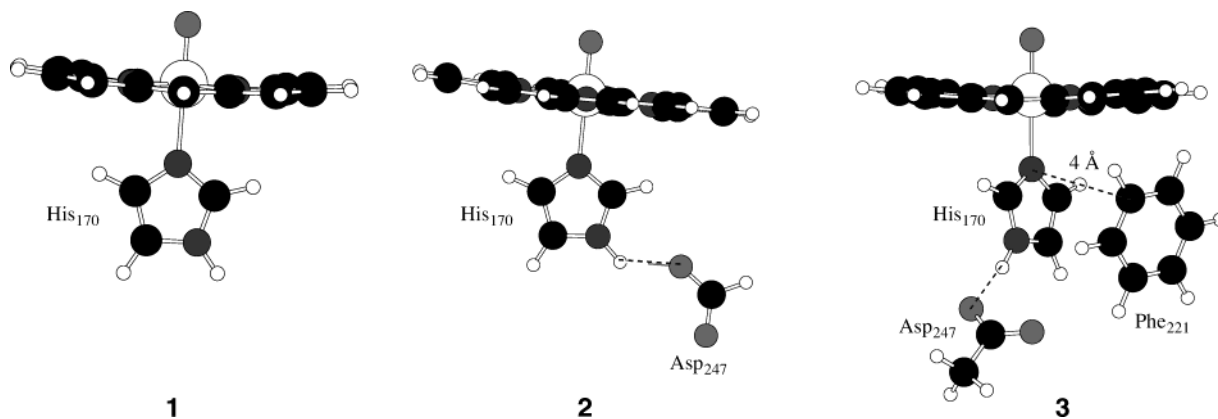
with an attempt to understand the similarities and differences between different Cpd I species.

During the 1980−1990s, there have been extensive discussions in the literature regarding the ground state of Cpd I of HRP. A combination of [17]O ENDOR[19] and ^{14}N ENDOR experiments[20] identified the ground state as having a triplet spin situation on the Fe^{IV}=O unit coupled to a doublet spin on the porphyrin ring that exists as a radical cationic species (i.e., Fe^{IV}-OPor$^{•+}$). Since strong resonances appeared on the pyrrole nitrogen atoms of the porphyrin, the ground state was assigned as the A$_{2u}$ state, in which the odd electron resides in the a$_{2u}$ orbital. Mössbauer spectra[21] support the assignment of spin coupling of an oxo-iron triplet with a porphyrin cation radical situation. In contrast to Hoffman et al.,[19,20] Kincaid et al.[22] assigned the ground state of Cpd I of HRP as a ^{2}A$_{1u}$ state based on resonance Raman spectra. Their spectra, however, showed strong sensitivity to the intensity of the laser beam. Resonance Raman spectra of Chuang and Van Wart[23] predicted a ^{2}A$_{2u}$ ground state in agreement with the EPR and ENDOR results of Hoffman and co-workers.[19,20] The active species of HRP was studied before by means of density functional theoretic (DFT) calculations, which generally show that the ground state is most likely the ^{4}A$_{2u}$ state derived from the Fe^{IV}OPor$^{•+}$ species.[4,24−29] Since the aspartate anion, in Scheme 1, may deprotonate the histidine ligand, most of these studies consider two optional situations for the proximal ligand, as a protonated imidazole (ImH) and as an imidazolate anion (Im$^-$). Deeth[27] used the BP86 functional and demonstrated that Cpd I(HRP) with either ImH or Im$^-$ ligands can undergo a facile saddling distortion that changes the spin density distribution of the ^{4}A$_{2u}$ state. Green[28] used the B3LYP functional and showed that ImH as a proximal ligand reproduced the experimental doublet-quartet splitting better than the anionic form Im$^-$. Harris and Loew[4b] showed that, in the presence of aspartate, the BPW91 calculated energy difference between the ImH (Asp$^-$) and Im$^-$(AspH) situations of the proximal ligand is extremely small (1 kcal mol^{-1}). Nevertheless, the protonated form of the ligand, ImH, was required to reproduce the spectral characteristics of Cpd I(HRP), and the corresponding differences compared with the P450 species. Deeth,[27] Harris and Loew,[4b] and Green[28] noted the drastic spin density redistribution that occurs when the imidazole ligand is deprotonated.

In C*c*P, the iron is also in oxidation state Fe^{IV} with the Fe−O moiety having a triplet spin; however, the third unpaired electron is not located on the porphyrin ring but in a π-orbital of the tryptophan amino acid (Trp$_{191}$).[30] The active species (so-called Cpd ES) of C*c*P was theoretically studied by Siegbahn and co-

(14) Poulos, T. L.; Coup-Vickery, J.; Li, H. In *Cytochrome P450: Structure, Mechanisms and Biochemistry*, 2nd ed.; Ortiz de Montellano, P. R., Ed.; Plenum Press: New York, 1995; Chapter 4, pp 125−150.
(15) Suzuki, N.; Huguchi, T.; Urano, Y.; Kikuchi, K.; Uekusa, H.; Ohashi, Y.; Uchida, T.; Kitagawa, T.; Nagano, T. *J. Am. Chem. Soc.* **1999**, *121*, 11571−11572.
(16) Ohno, T.; Suzuki, N.; Dokoh, T.; Urano, Y.; Kikuchi, K.; Hirobe, M.; Higuchi, T.; Nagano, T. *J. Inorg. Biochem.* **2000**, *82*, 123−125.
(17) (a) Ogliaro, F.; Cohen, S.; de Visser, S. P.; Shaik, S. *J. Am. Chem. Soc.* **2000**, *122*, 12892−12893. (b) Ogliaro, F.; de Visser, S. P.; Cohen, S.; Kaneti, J.; Shaik, S. *ChemBioChem* **2001**, 848−851.
(18) Schöneboom, J. C.; Lin, H.; Reuter, N.; Thiel, W.; Cohen, S.; Ogliaro, F.; Shaik, S. *J. Am. Chem. Soc.* **2002**, *124*, 8142−8151.

(19) Roberts, J. E.; Hoffman, B. M.; Rutter, R.; Hager, L. P. *J. Am. Chem. Soc.* **1981**, *103*, 7654−7656.
(20) Roberts, J. E.; Hoffman, B. M.; Rutter, R.; Hager, L. P. *J. Biol. Chem.* **1981**, *256*, 2118−2121.
(21) Schulz, C. E.; Rutter, R.; Sage, J. T.; Debrunner, P. G.; Hager, L. P. *Biochemistry* **1984**, *23*, 4743−4754.
(22) Kincaid, J. R.; Zheng, Y.; Al-Mustafa, J.; Czarnecki, K. *J. Biol. Chem.* **1996**, *271*, 28805−28811.
(23) Chuang, W.-J.; Van Wart, H. E. *J. Biol. Chem.* **1992**, *267*, 13293−13301.
(24) Loew, G. H.; Kert, C. J.; Hjelmeland, L. M.; Kirchner, R. F. *J. Am. Chem. Soc.* **1977**, *99*, 3534−3536.
(25) Du, P.; Loew, G. H. *Biophys. J.* **1995**, *68*, 69−80.
(26) Kuramochi, H.; Noodleman, L.; Case, D. A. *J. Am. Chem. Soc.* **1997**, *119*, 11442−11451.
(27) Deeth, R. J. *J. Am. Chem. Soc.* **1999**, *121*, 6074−6075.
(28) Green, M. T. *J. Am. Chem. Soc.* **2000**, *122*, 9495−9499.
(29) (a) Filatov, M.; Harris, N.; Shaik, S. *J. Chem. Soc., Perkin Trans. 2* **1999**, 399−410. (b) Anthony, J.; Grodzicki, M.; Trautwein, A. X. *J. Phys. Chem. A* **1997**, *101*, 2692−2701.

Scheme 2. Three Different Models of Cpd I of HRP Used in This Study

of the low-lying states of HRP under different environmental conditions. As this work shows, Cpd I of HRP indeed behaves as a chameleon species and its character is influenced by the environmental effects and, hence, may be manipulated by site directed changes in the protein environment.

Results and Discussion.

Based on the X-ray structure of Cpd I of HRP (see Scheme 1),[7,12] we tested the environmental effects in three different models, which are shown in Scheme 2. The first model, **1**, contains the oxo-iron porphyrin with imidazole as axial ligand replacing His$_{170}$; the second model, **2**, has an additional formate anion mimicking the Asp$_{247}$ amino acid side chain; and a third model, **3**, includes an acetate anion replacing Asp$_{247}$ and a benzene ring replacing Phe$_{221}$. The geometries of models **1** and **2** were fully optimized, whereas only single-point calculations on the geometry of model **3** of the X-ray structure (1HCH)[7,12] were performed; see Scheme 2.

Some high-lying occupied and low-lying virtual orbitals of Cpd I of HRP are depicted in Scheme 3. On the left-hand side are shown the orbitals of the FeO moiety and are labeled according to the iron 3d orbital terminology. The lowest one of those is the nonbonding δ ($d_{x^2-y^2}$) orbital, which lies in the plane of the porphyrin ring and is usually doubly occupied. Higher lying are two nearly degenerate π^* orbitals along the Fe$-$O axis, which are labeled π^*_{xz} and π^*_{yz} and involve antibonding interactions between the 3d$_{xz}$ (3d$_{yz}$) orbitals on iron with the 2p$_x$ (2p$_y$) atomic orbitals on oxygen. The π^*_{xz} orbital lies in the plane of the imidazole ring, while the π^*_{yz} is perpendicular toward the plane and, therefore, may in principle mix with the π-system of the imidazole ring. Two low-lying virtual orbitals are the σ^*_{xy} and $\sigma^*_{z^2}$ orbitals, which have antibonding Fe$-$N and Fe$-$O characters, respectively. On the right-hand side, we depicted two high-lying nonbonding porphyrin orbitals, which in D_{4h} symmetry have the labels a$_{2u}$ and a$_{1u}$. The total set of orbitals in Scheme 3 is filled with 7 electrons, an occupancy that fits the ^{4}A$_{2u}$ state, where the term symbol derives from the label of the singly occupied porphyrin orbital. Many variants of distributing the electrons over these orbitals were tested to screen candidate low-lying states and examine their ordering under perturbation of the environmental effects.

Ground State of Cpd I for HRP. The lowest-lying electronic states of model **1** in the gas phase were found to be ^{4,2}A$_{2u}$ and ^{4,2}A$_{1u}$. Both of these states have a δ^2 $\pi^*_{xz}{}^1$ $\pi^*_{yz}{}^1$ configuration in the FeO unit, which corresponds to a d^4 electronic config-

workers[31] using density functional theory (DFT). Their model system included the oxo-iron porphyrin unit, an imidazole ring instead of His$_{175}$, and a formate replacing the Asp$_{235}$ side chain, and an indole for Trp$_{191}$. They found that, in the quartet spin state, there were two spins located on the Fe$=$O unit, while a third spin was spread equally over the porphyrin ($\rho_{Por} = 0.48$) and indole ($\rho_{Indole} = 0.47$) groups.

A change of the electronic ground state under the influence of environmental effects was reported by Green who used B3LYP calculations.[32] He modeled Cpd I(CAT) with an oxo-iron porphyrin and phenolate as an axial ligand. Although the assigned ground state of Cpd I(CAT) is the ^{4}A$_{2u}$ state, Green's calculations of the bare system predicted a ^{2}A$_{2u}$ ground state. However, the addition of electrostatic interactions from either a methylguanidium ion or a potassium cation stabilized ^{4}A$_{2u}$ as the ground state, in agreement with experiment.

In recent work by our group[33] on the competition of hydroxylation and epoxidation of propene by a Cpd I model of P450, we showed that the addition of two NH- - -S hydrogen bonds to the thiolate sulfur changed the epoxidation/hydroxylation product ratio in favor of hydroxylation. Experimental data by Morishima et al.[34] showed that a site directed mutation that severed one of the NH- - -S hydrogen bonds in P450$_{cam}$ affected the activity of enzyme in a variety of ways (e.g., uncoupling and product formation rates), including its epoxidation/hydroxylation product ratio in its oxidation of cyclohexene. Obviously, the protein environment can be crucial for the correct description of the ground-state properties of Cpd I species.

As discussed above, the active species of HRP has been modeled before using a variety of theoretical methods.[24–28] The effect of the environment on the electronic states of the active species is, however, less known. And this is done in the present work, which constitutes an extensive theoretical investigation

(30) (a) Huyett, J. E.; Doan, P. E.; Gurbiel, R.; Houseman, A. L. P.; Sivaraja, M.; Goodin, D. B.; Hoffman, B. M. *J. Am. Chem. Soc.* **1995**, *117*, 9033–9041. (b) Bonagura, C. A.; Sundaramoorthy, M.; Pappa, H. S.; Patterson, W. R.; Poulos, T. L. *Biochemistry* **1996**, *35*, 6107–6115. (c) Bonagura, C. A.; Sundaramoorthy, M.; Bhaskar, B.; Poulos, T. L. *Biochemistry* **1999**, *38*, 5538–5545. (d) Bonagura, C. A.; Bhaskar, B.; Sundaramoorthy, M.; Poulos, T. L. *J. Biol. Chem.* **1999**, *274*, 37827–37833. (e) Bhaskar, B.; Bonagura, C. A.; Li, H.; Poulos, T. L. *Biochemistry* **2002**, *41*, 2684–2693. (f) Private communication by Poulos, T. L. to Shaik, S.
(31) Wirstam, M.; Blomberg, M. R. A.; Siegbahn, P. E. M. *J. Am. Chem. Soc.* **1999**, *121*, 10178–10185.
(32) Green, M. T. *J. Am. Chem. Soc.* **2001**, *123*, 9218–9219.
(33) (a) de Visser, S. P.; Ogliaro, F.; Sharma, P. K.; Shaik, S. *Angew. Chem., Int. Ed.* **2002**, *41*, 1947–1951. (b) de Visser, S. P.; Ogliaro, F.; Sharma, P. K.; Shaik, S. *J. Am. Chem. Soc.* **2002**, *124*, 11809–11826.
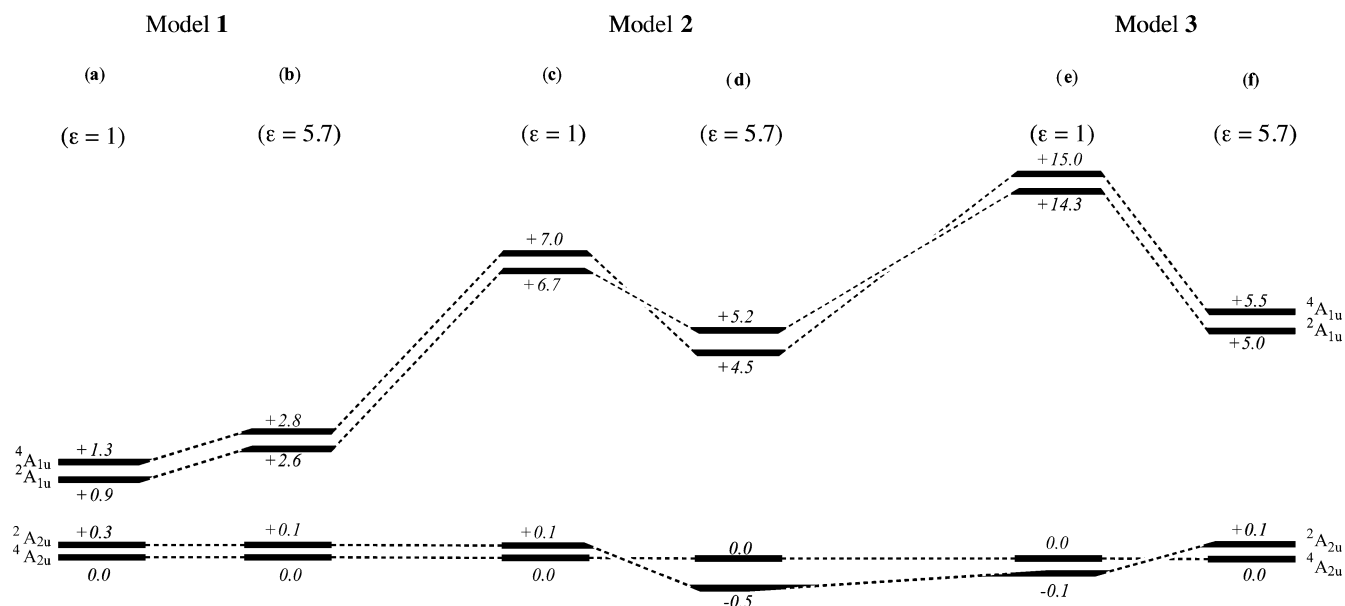(34) Yoshioka, S.; Takahashi, S.; Ishimori, K.; Morishima, I. *J. Inorg. Biochem.* **2000**, *81*, 141–151.

Model **1**   Model **2**   Model **3**

(a)   **(b)**   **(c)**   **(d)**   **(e)**   **(f)**

($\varepsilon = 1$)   ($\varepsilon = 5.7$)   ($\varepsilon = 1$)   ($\varepsilon = 5.7$)   ($\varepsilon = 1$)   ($\varepsilon = 5.7$)

Figure 1. Relative energies of the $^{4,2}A_{2u}$ and $^{4,2}A_{1u}$ states of Cpd I of HRP under different environmental conditions: (a) model **1** in the gas phase, (b) model **1** in a dielectric constant $\epsilon = 5.7$, (c) model **2** in the gas phase, (d) model **2** in a dielectric constant $\epsilon = 5.7$, (e) model **3** in the gas phase, (f) model **3** in a dielectric with $\epsilon = 5.7$. All calculations correspond to single-point LACV3P++** calculations on optimized LACVP+* geometries. Calculations in a dielectric with $\epsilon = 5.7$ used the LACVP+* basis set.

Scheme 3. High-Lying Occupied and Low-Lying Virtual Orbitals of Cpd I of HRP[a]
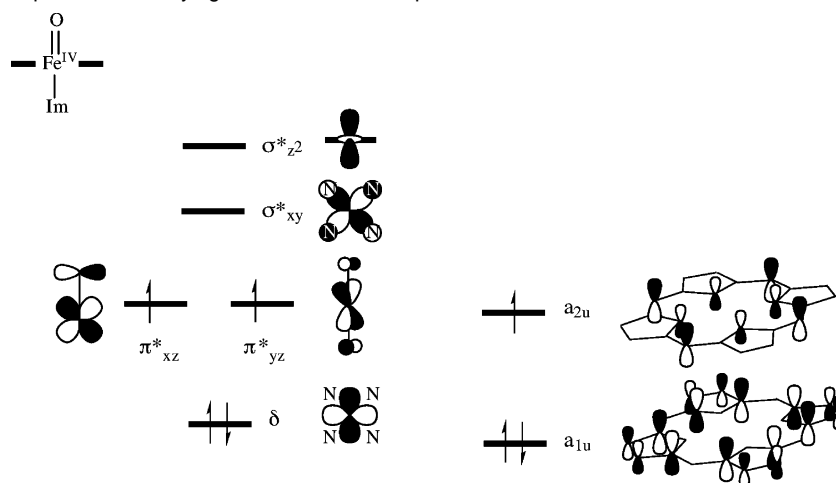
[a] The occupancy corresponds to the $^4A_{2u}$ State.

uration on iron and, hence, to an oxidation state Fe^{IV}. In addition, in both cases, there is a porphyrin hole in either the a_{2u} or a_{1u} orbitals. As shown in Figure 1, in the gas phase, all the four states are condensed within 1.3 kcal mol^{-1} of each other. As found already by Green,[28] the energy difference between $^4A_{2u}$ and $^2A_{2u}$ is small, ca. 0.3 kcal mol^{-1}, in favor of the high-spin (HS) state. Kuramochi et al.[26] calculated a larger energy gap, between the $^4A_{2u}$ and $^4A_{1u}$ states, of 3.5 kcal mol^{-1}. This rather large difference arises, probably, since the latter authors did not perform geometry optimizations but did single-point calculations on the X-ray structure only. Nevertheless, their state ordering is in agreement with our results here.

In addition to the $^{4,2}A_{2u}$ and $^{4,2}A_{1u}$ states, we tested a few more low-lying states. The $^6A = \delta^1 \pi^*_{xz}{}^1 \pi^*_{yz}{}^1 \sigma^*_{xy}{}^1 a_{2u}{}^1$ state, was found to be much higher in energy, 12.8 kcal mol^{-1} above the $^4A_{2u}$ state in the gas phase (in model **1**). The $^2\Pi_{xz}$ state ($\delta^2 \pi^*_{xz}{}^1 \pi^*_{yz}{}^0 a_{2u}{}^2$) with the iron in the oxidation state Fe^V is 28.2 kcal mol^{-1} above the $^4A_{2u}$ state. Likewise, a $^4\Pi_{Im}$ state ($\delta^2 \pi^*_{xz}{}^1$

$\pi^*_{yz}{}^1 a_{2u}{}^2 \pi_{Im}{}^1$) with an Fe^{IV} situation and a radical located on the imidazole ring rather than on the porphyrin ring is 34.3 kcal mol^{-1} higher. Since these three states were substantially higher in energy than the ground state in model **1**, we did not pursue them, any longer, in the larger models.

Figure 1 shows the relative energies of the $^{4,2}A_{2u}$ and $^{4,2}A_{1u}$ states of the Cpd I models for HRP in the gas phase and in a polarizing medium with a dielectric constant, $\epsilon = 5.7$. As can be seen from Figure 1, all models predict the $^{4,2}A_{2u}$ states to be an almost degenerate set of ground electronic states. In the larger systems, in **2** under polarized environment conditions, we find a $^2A_{2u}$ ground state, while the results for **3** indicate a $^4A_{2u}$ ground state; these results are in agreement with experimental ENDOR assignments, which show an A$_{2u}$ state with a small ferro−antiferromagnetic splitting.[19,20] In the smallest system in the gas phase, the $^{4,2}A_{1u}$ states are only 0.9−1.3 kcal mol^{-1} higher in energy than the $^4A_{2u}$ state, but, in the bigger models, the separation becomes significantly larger. Especially, in **3**, the

separation between the A_{2u} and A_{1u} states rises steeply to 14–15 kcal mol^{-1}. The $^{4,2}A_{1u}$ states, however, are seen to be more sensitive than the A_{2u} states to the polarity of the environment, and the energy gap between the $^4A_{2u}$ and $^4A_{1u}$ states drops, by 9.5 kcal mol^{-1}, to 5.5 kcal mol^{-1} with inclusion of polarity ($\epsilon = 5.7$). Therefore, it may very well be that mimetic complexes in a strongly polar solvent may have a $^{2,4}A_{1u}$ ground state. However, in the protein pocket, in the presence of amino acid residues such as Asp, Trp, etc., which are electron-rich and polarizable amino acids, the ground state is clearly $^{2,4}A_{2u}$.

In the gas phase in model **1**, the energy gap between the A_{1u} and A_{2u} states is much lower than the one obtained for Cpd I of P450, where the gap was larger than 20 kcal mol^{-1}.[35] The reason for this is the "push effect" of the thiolate ligand.[36] In P450, the doubly occupied σ-sulfur orbital of the thiolate ligand interacts strongly with the a_{2u} porphyrin orbital that acquires an antibonding character and rises in energy relative to the a_{1u} orbital. This widens the energy gap between the A_{2u} and A_{1u} states and favors single occupation of a_{2u} over the a_{1u} orbital. The mixing of the σ-hybrid of the axial ligand with the a_{2u} orbital is negligible or absent in the case of a weak electron donor ligand like imidazole, and therefore the A_{2u} and A_{1u} electronic states are almost degenerate as is the case in an isolated porphyrin molecule.[37] Thus, a strong "push effect" of the ligand is expected to lower the electron affinity of Cpd I considerably. To validate this, we calculated the lowest lying states of HRP Cpd II, i.e., the one electron reduced form of Cpd I. In principle, filling the porphyrin hole of the $^{4,2}A_{2u}$ and $^{4,2}A_{1u}$ states of Cpd I gives the same Cpd II state with a $^3\Pi = \pi*_{xz}{}^1 \pi*_{yz}{}^1 a_{2u}{}^2 a_{1u}{}^2$ configuration. In the gas phase (model **1**), we find an electron affinity of 6.41 eV from Cpd I in the $^4A_{2u}$ state. As expected, this value is substantially larger than the one obtained for P450 due to the cysteinate "push effect", where a value of 3.06 eV was obtained.[36] Since the exothermicity of electron acceptance by Cpd I to produce Cpd II in HRP is much larger than in P450, this means *that HRP will participate in electron transfer reactions more readily than P450*, and may function as a better electrophile in oxygen transfer reactions. Experimentally, HRP models and peroxidases participate in electron-transfer (ET) reactions, e.g., with phenols,[2e] during dealkylation of amines[38] and sulfoxidation.[39] By comparison, the role of ET in P450 is questionable,[2a] and a recent study[40] provides strong evidence disfavoring electron transfer during P450 dealkylation of secondary amines which are characteristic electron-transfer probe substrates, e.g., *N*-cyclopropyl-*N*-methylaniline. There are no systematic studies of relative rates of, e.g., epoxidation, hydroxylation, and other oxygen-transfer reactions for HRP vis-à-vis P450. However, HRP type complexes are known to be better epoxidating agents than P450s.[15,16]

(35) Ogliaro, F.; de Visser, S. P.; Groves, J. T.; Shaik, S. *Angew. Chem., Int. Ed.* **2001**, *40*, 2874–2876; erratum *ibid.* 3503.
(36) Ogliaro, F.; de Visser, S. P.; Shaik, S. *J. Inorg. Biochem.* **2002**, *91*, 554–567.
(37) Ghosh, A. *Acc. Chem. Res.* **1998**, *31*, 189–198.
(38) (a) Karki, S. B.; Dinnocenzo, J. P.; Jones, J. P.; Korzekwa, K. R. *J. Am. Chem. Soc.* **1995**, *117*, 3657–3664. (b) Goto, Y.; Watanabe, Y.; Fukuzumi, S.; Jones, J. P.; Dinnocenzo, J. P. *J. Am. Chem. Soc.* **1998**, *120*, 10762–10763. (c) Goto, Y.; Matsui, T.; Ozaki, S.-I.; Watanabe, Y.; Fukuzumi, S. *J. Am. Chem. Soc.* **1999**, *121*, 9497–9502.
(39) Goto, Y.; Matsui, T.; Ozaki, S.-I.; Watanabe, Y.; Fukuzumi, S. *J. Am. Chem. Soc.* **1999**, *121*, 9497–9502.
(40) Shaffer, C. L.; Harriman, S.; Koen, Y. M.; Hanzlik, R. P. *J. Am. Chem. Soc.* **2002**, *124*, 8268–8274.

Geometric Features of Cpd I for HRP. The optimized geometries of **1** and **2** in the $^{4,2}A_{2u}$ and $^{4,2}A_{1u}$ states are depicted in Figure 2. Some geometric changes are observed after the addition of a formate anion to the model. In the $^{4,2}A_{2u}$ states, the Fe–O distance enhances slightly to 1.625 Å, while the Fe–N_{ImH} distance to the imidazole ligand shortens to 2.158 (HS) and 2.160 (LS) Å. For the $^{2,4}A_{1u}$ states, the geometric effect is more pronounced and the Fe–N_{ImH} distance shortens significantly, e.g., from 2.203 Å to 2.143 Å (HS), with a concomitant, albeit smaller, lengthening of the FeO bond from 1.618 to 1.62 Å (HS). This is the well-known *trans* effect,[41] and one might argue that the aspartate anion in the protein pocket serves to stabilize the Fe–N_{ImH} linkage. Our calculated geometries[4] of the $^{4,2}A_{2u}$ states compare reasonably well with the experimentally obtained structures of HRP Cpd I,[5–7] C*c*P Cpd ES,[9] and myoglobin (Mb) Cpd I.[42] The comparison in Table 1 shows that the experimental Fe–O distances of the histidine ligated species range from 1.62 to 1.70 Å, while we find 1.620–1.625 Å (Figure 2). These values of the Fe–O distance are typical for an Fe=O double bond and very similar in value to the ones we obtained with a P450 model with thiolate as axial ligand, where we found Fe–O distances of 1.651 Å (HS) and 1.648 Å (LS).[35] The most significant difference between the P450 and HRP models is the displacement of the iron atom from the porphyrin plane, Δ. Due to the "push effect" of the thiolate ligand, the iron is lying much more above the plane of the porphyrin ring, namely $\Delta = 0.143$ Å (HS) and 0.154 Å (LS).[35] In the HRP models in Figure 2 (and Table 1), the value of Δ is much smaller, i.e., 0.078 Å. The experimentally obtained Fe–N_{his} distances for Cpd I of HRP vary over a relatively large range from 1.93 Å for HRP Cpd I[5] to 2.10 Å in the most recent work.[7] Our theoretical value of 2.158–2.175 Å is closer to the latter one. It is still however on the longish side relative to experiment.

Chameleon Features of Cpd I for HRP. The group spin densities of the $^4A_{2u}$ and $^4A_{1u}$ states of models **1**, **2**, and **3** in the gas phase and with a dielectric constant of $\epsilon = 5.7$ are indicated in Figure 3. The spin densities of the low-spin species are similar to the ones obtained for the high-spin and are omitted from the figure. These as well as the group charges exhibit the same trend as the spin densities of the HS states and hence are relegated to the Supporting Information. As shown in the figure, electronically, there are significant differences between the results for **1**, on one hand, and **2** and **3**, on the other. Thus, while in all models, in the $^{4,2}A_{2u}$ states as well as in the $^{4,2}A_{1u}$ states, the spin densities on the FeO unit are approximately 2 corresponding to singly occupied $\pi*_{xz}$ and $\pi*_{yz}$ orbitals, the distribution of the third spin shows sensitivity to the environment of Cpd I. This remaining spin density is expected to reside on the porphyrin ring due to single occupation of the a_{1u} or a_{2u} orbitals. Initially, in the smallest system (**1**), this is indeed the case, where, in the A_{2u} state, a spin density of almost unity resides on the porphyrin ring, with very small residual density on the imidazole axial ligand. Addition of the carboxylate species in **2** and **3** removes part of the spin density from the

(41) (a) Hildebrand, D. P.; Ferrer, J. C.; Tang, H.-L.; Smith, M.; Mauk, A. G. *Biochemistry* **1995**, *34*, 11598–11605. (b) Decatur, S. M.; Franzen, S.; DePillis, G. D.; Dyer, R. B.; Woodruff, W. H.; Boxer, S. G. *Biochemistry* **1996**, *35*, 4939–4944.
(42) Chance, M.; Powers, L.; Kumar, C.; Chance, B. *Biochemistry* **1986**, *25*, 1259–1265.
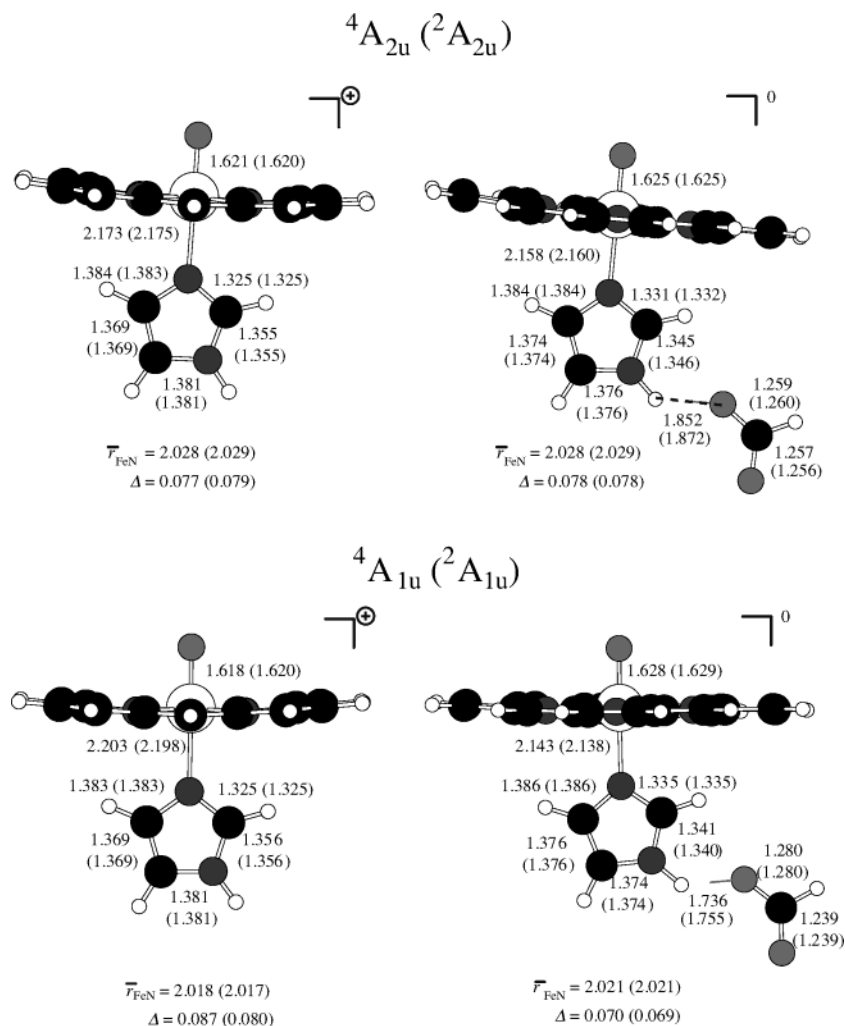
$$^4A_{2u} \; (^2A_{2u})$$

$$^4A_{1u} \; (^2A_{1u})$$

Figure 2. Optimized geometries at the B3LYP/LACVP+* level of theory of **1** (left side structures) and **2** (right side structures) in the $^{4,2}A_{2u}$ and $^{4,2}A_{1u}$ states. The data in parentheses refer to the low-spin state.

Table 1. Experimental and Theoretical Bond Lengths of the Active Species of Some Heme-Containing Enzymes

	Fe–O	Fe–N_{his}	Fe–N_{por}	Δ^a	reference
HRP Cpd I	1.64	1.93	2.02		5
HRP Cpd I	1.62–1.64		2.00		6
HRP Cpd I	1.7	2.1			7
HRP Cpd I	1.620–1.625	2.158–2.175	2.028–2.029	0.078	this work[b]
CcP Cpd ES	1.67 ± 0.04	1.91 ± 0.03	2.02 ± 0.02		9
Mb Cpd I	1.69	2.11	1.98		42
P450 Cpd I; HS	1.651		2.017	0.143	35
P450 Cpd I; LS	1.648		2.017	0.154	35
P450 Cpd I; LS	1.65		2.02		48
P450 Cpd I; HS	1.642				49
P450 Cpd I; LS	1.642				49

^{a} Δ is the displacement of the iron atom with respect to the porphyrin plane. ^{b} The values for Fe–O, Fe–N_{his}, and Fe–N_{por} bond distances depicted here represent the minimum and maximum values obtained for the A_{2u} states of **1** and **2** from Figure 2.

porphyrin ring. For instance, in the $^4A_{2u}$ state, the spin density on the porphyrin is $\rho_{Por} = 0.95$ in **1** but only 0.55 in **2** with the remainder located on the formate; $\rho_{Form} = 0.40$. Thus, while **1** contains a porphyrin cation radical situation, the porphyrin in **2** is only partially charged and so is the formate; i.e., **2** is in a $Por^{\delta \bullet +}$ $Form^{\delta-}$ situation, rather than in a $Por^{\bullet +}$ $Form^-$ situation. The same happens in system **3** where in the gas phase the spin densities are spread out over the porphyrin and the formate in the A_{2u} states, while the phenyl group of the Phe residue

(mimicked by benzene) is merely a spectator. In a polar environment with a dielectric constant of 5.7, the separation of spin and charge in the $^{4,2}A_{2u}$ states, however, disappears again and the spin densities become purely porphyrin-based, whereas the formyl species is purely anionic. Obviously, in the gas phase, charge separated systems are less favorable than in a polar environment (mimicked by the dielectric constant). This again points out the importance of including environmental effects.

By contrast to A_{2u}, in the A_{1u} states, in all models, the a_{1u} spin densities are located on the porphyrin ring only and the formate remains purely anionic throughout. This does not change with the presence of benzene or with the application of a dielectric environment. Thus, as we change from **1** to **2** and **3**, the A_{1u} states remain in the $Por^{\bullet +}$ $Form^-$ situation. Consequently, the application of a dielectric constant stabilizes the A_{1u} state relative to A_{2u}, and this differential stabilization is larger for **2** and **3**, where the gas-phase systems have small charge separation. Thus, while a dielectricon is a crude approximation to the electric field of the protein, we expect that the changes in the A_{2u}–A_{1u} energy gaps will exhibit similar trends in a realistic calculation including the protein. The tendency of the A_{2u} state to delocalize its spin, by contrast to the A_{1u} state that does not, underscores the importance of the
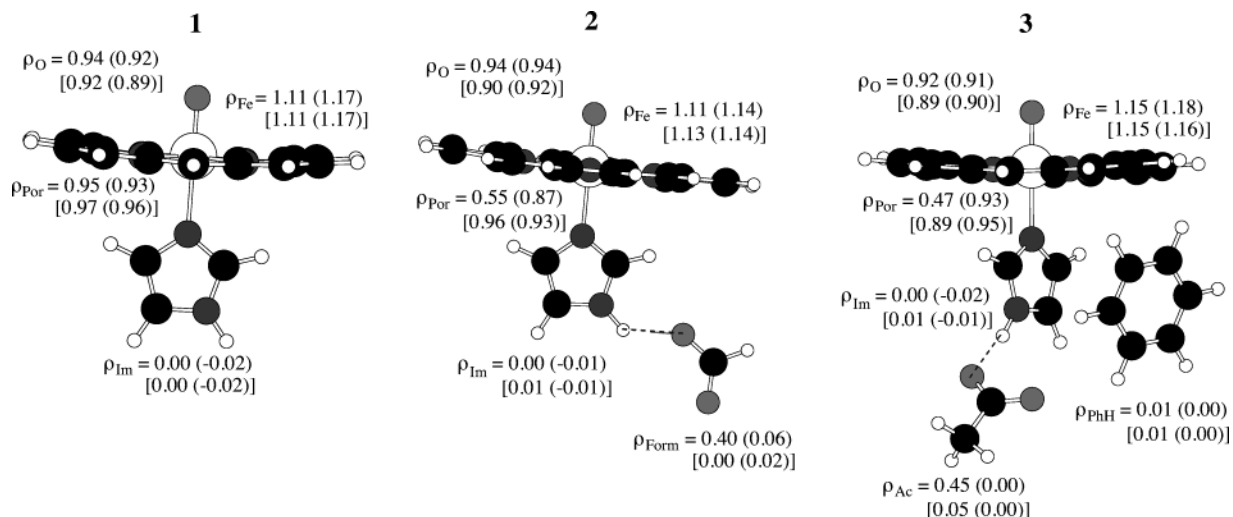
Figure 3. Group spin densities (ρ) for the three models **1**, **2**, and **3** in the $^4A_{2u}$ and $^4A_{1u}$ states in the gas phase and in a dielectric constant of $\epsilon = 5.7$. The data are organized as follows: out of parentheses for A_{2u}, inside parentheses for A_{1u}, in square brackets are the data with application of a dielectric constant of 5.7, while out of brackets are data for gas-phase calculations ($\epsilon = 1$). Calculations in the gas phase were performed with the LACV3P++** basis set and in $\epsilon = 5.7$ with the LACVP+* basis set.

Table 2. Experimental[a] and Calculated[b] Adiabatic Ionization Energies (IP) of Some Amino Acid Side Chain Models[c]

species	theory[b]	experiment[a]
benzene	8.96	9.24
toluene	8.54	8.83
p-methyl phenol	7.90	8.34
indole	7.51	7.76
indolide	2.31	2.52
p-methyl phenolate	2.03	2.17
PorH$_2$		6.90
SH$^-$	2.34[d]	
SCH$_3^-$	1.86[d]	
SCys$^-$	2.61[d]	
ImH	10.19[e]	
Cpd II of HRP	6.41[f]	
Cpd II of P450	3.06[e,f]	
Cpd II (no proximal ligand)	7.09[e,f]	

[a] Taken from the NIST database (ref 43). [b] Energies include zero-point corrections and were calculated with B3LYP/LACVP+*. [c] All values are in eV. [d] From ref 50. [e] From ref 36. [f] IP$_{Cpd\ II}$ = EA$_{Cpd\ I}$.

orbital overlap between the side chains and the singly occupied porphyrin based orbitals, which only in the case of a$_{2u}$ extend to the axial ligand.[4a]

How can we understand all these fluctuations in the nature of the Cpd I species? What is the difference between Cpd I species of P450, CAT, HRP, and C*c*P? What is the reason that C*c*P has the radical located on a tryptophan amino acid,[2e,30] while in HRP and P450 the radical is located on the porphyrin ring? To assist the discussion, we collected in Table 2 calculated and experimental values[43] of ionization potential (IP) for molecules, which mimic the amino acid side chains of phenylalanine, tyrosine, and tryptophan, as well as some of porphyrin and the axial ligands.

Figure 4 shows a valence bond (VB) model, which has been used before to analyze the behavior of Cpd I(P450)[17,18] and which provides a simple rationale for the aforementioned group of Cpd I species. The VB model constructs the electronic structure of Cpd I species using two VB forms, one labeled
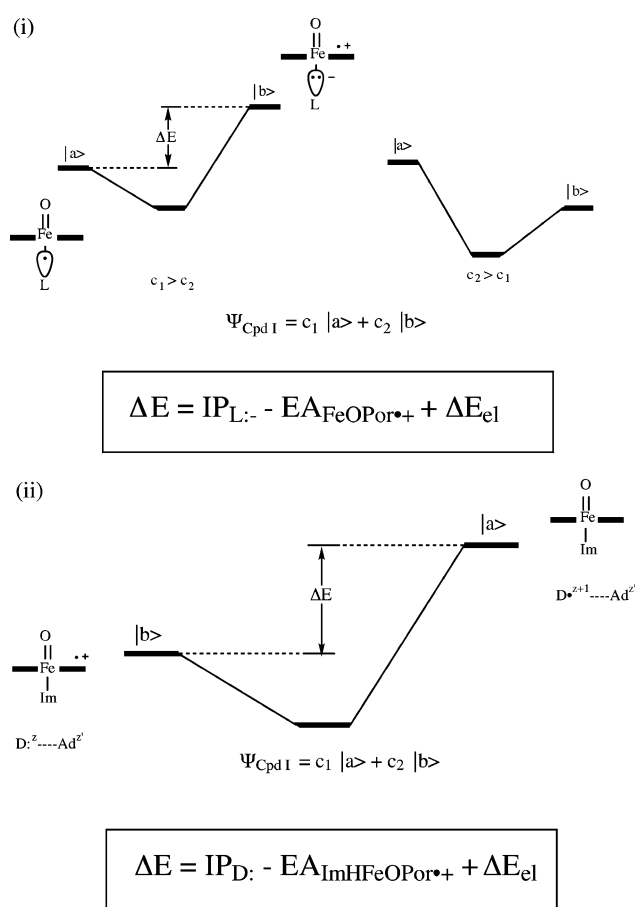
(43) Linstrom, P. J., Mallard, W. G., Eds. *NIST Chemistry Webbook*; NIST Standard Reference Database Number 69, March 2003, National Institute of Standards and Technology: Gaitherburg, MD, 20899 (http://webbook.nist.gov).

Figure 4. Valence bond description of the mixing of a porphyrin cation radical situation with a closed shell porphyrin but with the radical either on the axial ligand L$^\bullet$ (i) or on an adjacent side chain residue D$^\bullet$ (ii). See text for explanation.

$|a>$ has a closed shell porphyrin (Por) and a radical on the axial ligand (L$^\bullet$) or on an adjacent side chain residue (D$^\bullet$); the other form labeled $|b>$ has a porphyrin radical cation situation (Por$^{\bullet+}$). The mixing of these two VB forms gives rise to the state of Cpd I that has a mixed character, which depends inter alia on the relative energy of the two forms. Of course, the use of two

forms is a matter of convenience and should not be taken in a restrictive sense; *there can be three, four, or more VB forms, depending on the number of residues or substituents that can participate in electron donation to the Por$^{\bullet+}$ species*. Thus, for example, the propionate substituents on the porphyrin (Scheme 1) are such potential donors, and whenever not screened properly by salt bridges, they may well participate in the electron donation to Por$^{\bullet+}$.

The energy gap between the forms is given by the difference between the IP of the donor group (L: or D:) and the electron affinity (EA) of the FeOPor$^{\bullet+}$ species and the difference in electrostatic interaction energy (ΔE_{el}) in the two forms. A strong condition for the efficient mixing of the VB forms is that they maintain a finite orbital overlap. *Without such an overlap, Cpd I will assume the character of the lowest energy form, and the radical will be transferred to the most "stable" site*. In the case where the axial ligand is the donor, the overlap requirement is met. However, in the case where the donor is a side chain residue, this overlap will be rather weak and the orientation of the donor relative to Cpd I may be crucial for mediating some overlap that will enable the mixing of the forms.

Figure 4 consists of two mixing diagrams, (i) and (ii), which differ by the identity of the donor. In (i), we describe cases where the axial ligand is a good enough electron donor, like thiolate or tyrosynate (low IP, see Table 2), and can therefore participate in the electronic reorganization between the VB forms. Here, the form |b> is an ion pair, and the energy gap between the forms is modulated by hydrogen bonding to the axial ligand, by interaction with positively charged residues and by the polarity of the pocket, which together stabilize form |b> preferentially over |a>. In the gas phase, form |b> is above |a>, and hence, the mixed state has a predominant radical character on the ligand L.[17] However, within the protein pocket, the ion pair form is stabilized and descends below |a>, thereby creating a Cpd I state with a higher Por$^{\bullet+}$ character ($c_2 > c_1$). This behavior was elaborated for Cpd I(P450) of P450 and was reproduced in QM/MM calculations.[18] The results of Green[32] for Cpd I(CAT), in the gas phase and in the presence of positive ions, follow a similar trend. Furthermore, any unscreened anionic group in the pocket may compete with the axial ligand on electron donation to the porphyrin hole. This may happen either by participating in the electron structure through the mixing of additional VB forms of the |a>-type (Figure 4 (i)), having the radical species on the side chain residue, or by simply transferring an electron to the porphyrin hole to create a protein-centered radical. Thus, it was reported recently[44] that the active species of P450 transfers the spin to a tyrosine unit very quickly. Since the IP of *p*-methyl phenol (Table 2) is too high for an exothermic electron transfer to Cpd I, this implies that there are deprotonated tyrosine amino acids available which can transfer an electron to Cpd I. This, however, need not be a strict condition in HRP and other peroxidases where the electron affinity of the ImHFeOPor$^{\bullet+}$ species is high.

The diagram in (ii) corresponds to the situation in HRP and C*c*P where the axial ligand is the side chain imidazole, which is a poor electron donor with a relatively high IP (Table 2). In this case, the axial ligand cannot participate in electron donation

to the Por$^{\bullet+}$, and the FeOPor$^{\bullet+}$ form, |b>, is the lowest energy structure. However, since the ImHFeOPor$^{\bullet+}$ moiety is a very good electron acceptor (Table 2), side chain residues, which are good electron donors, designated as D:^{z}, *z* being the charge of the donor, and which can maintain some overlap disposition with ImHFeOPor$^{\bullet+}$, can participate in the electronic reorganization by mixing into the form |b>, where the heme moiety is now in the form LFeOPor and D appears in its radical form (D$^{\bullet z+1}$). The contribution of form |a> to the state of Cpd I can be assisted if in the proximity of the donor there exists additional charged groups, labeled as Ad$^{z'}$ (z' = charge), which can stabilize the radical form D$^{\bullet}$ in |a> and lower its energy gap with |b>. The situation devoid of Ad$^{z'}$ is our model system **2** (Scheme 2) where the sole donor is an aspartate anion (mimicked by formate). As can be gleaned from Figure 3, in the gas phase the forms |a> and |b> are almost equi-energetic, so that almost half of the spin density resides on the formyl residue. However, as soon as the effect of the pocket polarity is introduced, structure |b> where the localized formate anion is present is stabilized relative to form |a> and the mixing becomes minimal reducing the formyl spin density to zero. This abrupt annihilation of the mixing is a result of the poor orbital overlap between the formate and imidazole moieties.

In model system **3**, there is an additional potential donor, which is benzene that mimics the phenyl side chain of Phe. However, as seen in Table 2, benzene (and also toluene) is a poor electron donor, and hence the mixing of form |a> into |b> remains very small and **3** still resembles model system **2**. By contrast, as reported by Siegbahn et al.,[31] in the case of C*c*P, the additional group is the indole side chain of Trp$_{191}$, which is a much better electron donor than benzene (see Table 2). Now, Trp$_{191}$ can participate in the electron donation to the ImHFeOPor$^{\bullet+}$ moiety. The difference between the ionization potential of Trp and the electron affinity of ImFeOPor$^{\bullet+}$ is 1.1 eV (25.4 kcal mol^{-1}), and this difference is compensated by the electrostatic stabilization in the Asp^{-} Trp$_{191}^{\bullet+}$ pair. The results of Siegbahn et al.[31] indicate that the compensation is perfect, leading to equal partition of the radical between Por and Trp$_{191}$, in the gas phase. Reversal of the role, in which aspartate will donate an electron to the porphyrin hole, would have annihilated the charge stabilization in |a> and hence be much less favorable and not observed. Similarly, there exists another tryptophan in C*c*P above the porphyrin ring in the distal side (Trp$_{51}$ at the Fe=O side[2e,30]), but since it cannot enjoy the stabilization from an Asp anion, it does not donate an electron to the Por$^{\bullet+}$. As such, Cpd I(C*c*P) will have a significant Trp$_{191}^{\bullet+}$ character, which may be further enhanced by the polarity of the pocket. Since it is very likely that the Trp$_{191}$ and ImH moieties have a rather poor orbital overlap, the mixing may altogether drop to zero, and the radical will reside on the more stabilized site; namely an electron-transfer process from Trp to Por$^{\bullet+}$ will take place and may be attended by some reorganization of the environment to stabilize the newly formed Trp$^{\bullet+}$ site and minimize the orbital overlap even further. This appears to be the actual situation of Cpd I(C*c*P) in which the radical appears to be exclusively on Trp$_{191}^{\bullet+}$.[30a]

Thus, the VB model clarifies the difference between Cpd I(C*c*P) and Cpd I(HRP). In the case of Cpd I(HRP), the only potential donor to the porphyrin hole is the phenyl group of Phe, which is a poor electron donor, and hence Cpd I(HRP) is

(44) (a) Schünemann, V.; Jung, C.; Trautwein, A. X.; Mandon, D.; Weiss, R. *FEBS Lett.* **2000**, *479*, 149−154. (b) Schünemann, V.; Jung, C.; Terner, J.; Trautwein, A. X.; Weiss, R. *J. Inorg. Biochem.* **2002**, *91*, 586−596.

expected to be mostly an ImHFeOPor$^{\bullet+}$ type. By comparison, in Cpd I(C*c*P) there is an indole side chain of Trp$_{191}$, which is a good electron donor, and which by electron donation can be stabilized by the negatively charged aspartate. As such, Cpd I(C*c*P) will have a mixed character between the forms (Asp$^-$ Trp$_{191}$$^{\bullet+}$)ImHFeOPor and (Asp$^-$ Trp)ImHFeOPor$^{\bullet+}$, the former form being accentuated by the polarity of the pocket. However, as noted by Poulos et al.,[30b] in ascorbate peroxidase (APX), Cpd I(APX) is virtually (Asp$^-$ Trp)ImHFeOPor$^{\bullet+}$ despite the presence of Trp and Asp$^-$. One destabilizing factor in APX is a potassium cation, K$^+$, which is located 8 Å from the Trp residue and electrostatically destabilizes the Trp$^{\bullet+}$ species. However, there are additional differences, like the lesser polarity of the Trp environment in APX vs CcP,[30b] which contribute to the lack of Trp$^{\bullet+}$ species in APX. The chameleon nature of Cpd I(C*c*P) was beautifully demonstrated by Poulos et al.,[30b−e] who mutated C*c*P to involve the K$^+$ binding site. The mutation was indeed found to decrease the stability of the Trp$_{191}$$^{\bullet+}$ species. Other mutations of C*c*P caused Trp$_{191}$$^{\bullet+}$ to disappear, altogether, however with no concomitant appearance of a Por$^{\bullet+}$ species; the observed species was Cpd II which may have been formed by electron transfer from any number of species, including tyrosinates and possibly also the relatively unscreened propionate substituents of the porphyrin in C*c*P.[30f] Apparently, as deduced by Poulos,[2e,30] the nature of Cpd I is affected by subtle changes in the electrostatic and dipolar environment of the protein pocket. Clearly, other mutations (e.g., of the Asp residue, etc) that make use of the chameleonic behavior of Cpd I can be designed by manipulating the polar environment of the species.[30e] One possible challenge is the design of groups that can maintain a good orbital overlap (with the histidine or the heme moiety) and can thereby form a Cpd I species in which the radical is truly delocalized in a mixed state.

Summary

Cpd I species having histidine as a proximal ligand are, much like the Cpd I of P450, chameleon species in which the electronic structure varies with the nature of the protein environment that accommodates the species. A simple model is constructed that enables one to understand the various manifestations of this nature.[17,18] The model relies on the resonance mixing of the DFePor$^{\bullet+}$ and D$^{\bullet+}$FePor (D, donor residue) electronic forms, the effect of polarity on this mixing, and the overlap requirement between the residue, D, and the proximal ligand or the porphyrin of the heme moiety. In P450 and CAT, the proximal ligands, which are negatively charged, take the role of the donor residue and create species having mixed porphyrin radical cationic and ligand radical characters. The balance of these contributions will depend on the polarity, ionic strength, and hydrogen bonding capability of the protein environment.[4a,17,18,30b−f,32] For HRP, which does not possess a powerful electron donor in the proximal pocket, the lowest lying states are derived from the ^{4,2}A$_{2u}$ situations, which are very close in energy. Slightly higher in energy are a set of ^{4,2}A$_{1u}$ electronic states, which drop considerably in energy when a dielectric constant is applied. However, since the Por$^{\bullet+}$ moiety is a powerful electron acceptor, side chain amino acid residues that are sufficiently good electron donors can participate in the electronic structure by donating electron density to the Por$^{\bullet+}$ moiety. This is reflected in the structure of Cpd I for C*c*P, in which the radical species resides on Trp side chain. However,

as shown by Poulos et al.,[30b−f] relatively minor variations in the protein environment can shift the radical cationic species around.

Thus, nature has created enzymes that look very similar but nevertheless behave like chemical chameleons in which small changes to the environment can give totally different chemical properties of the active species. This sensitivity to the environment arises because the electronic structure of Cpd I, with a hole on the porphyrin, creates with various electron donors a scenario of a mixed-valent compound that can delocalize (or relay) its initial porphyrin hole to a variety of groups, in a manner that is sensitive to noncovalent interactions. It appears therefore that different heme-containing enzymes with small differences in local environments will have different electronic configurations and may show different catalytic behavior due to their chameleonic character. A proof of principle was given in the case of P450 where the chameleonic nature of Cpd I affects the relative reactivity of C−H vs C=C.[33,34] In the case of C*c*P, which participates in electron-transfer reactions, Poulos et al.[30] showed that minor alternations in the proximal pocket have drastic influences on the ability of Cpd I to transfer an electron. If this is a general trend, *then nature has found an economical way to generate enzymes with active species that have fixed chemical constitution but a variable nature and reactivity that derives from the variability of the protein environment*. Having said that, one must keep in mind that the catalytic activity is determined by an interplay of the electronic features of Cpd I and a variety of other factors, such as substrate bonding, the accessibility of the substrate to the active species, and so on.[45] Resolution of this interplay is the challenge for future studies.

Methods

All calculations were performed using the Jaguar 4.1 program package[46] and employed the unrestricted hybrid density functional method UB3LYP.[47] Models **1** and **2** were fully optimized with the LACVP+* basis sets, which consist of a Los Alamos type double-ζ quality basis set on Fe and a Pople type 6-31+G* basis set on all other atoms. Additional single-point calculations were performed with the triple-ζ quality LACV3P++**/6-311++G** basis set, which was buttressed with diffuse and polarization functions on all atoms. Solvent effect calculations were done with the Polarized Continuum Model (PCM) as implemented in Jaguar 4.1 with the dielectric constant ϵ = 5.7.

The active site of HRP Cpd I was modeled by taking an oxo-iron porphyrin group with an imidazole axial ligand in the place of the histidine side chain. Harris and Loew[4b] and Green[28] showed that imidazole is a much better mimic for Cpd I than imidazolate. With an imidazole ligand, the system has an overall charge of +1. In a second and larger model, we take an additional formate anion from an aspartic acid residue (Asp$_{247}$). Finally, in a third model, we took the X-ray geometry of 1HCH pdb[12] and did single-point calculations on the active site containing oxo-iron porphyrin, the imidazole group of His$_{170}$, the acetate group of Asp$_{247}$, and a benzene group for Phe$_{221}$. We modeled

(45) Park, J.-Y.; Harris, D. L. *J. Med. Chem.* **2003**, *46*, 1645−1660.
(46) *Jaguar 4.1*; Schrödinger, Inc.: Portland, OR, 2000.
(47) (a) Becke, A. D. *J. Chem. Phys.* **1993**, *98*, 5648−5652. (b) Becke, A. D. *J. Chem. Phys.* **1992**, *96*, 2155−2160. (c) Becke, A. D. *J. Chem. Phys.* **1992**, *97*, 9173−9177. (d) Lee, C.; Yang, W.; Parr, R. G. *Phys. Rev. Lett.* **1988**, *37*, 785.
(48) Green, M. T. *J. Am. Chem. Soc.* **1999**, *121*, 7939−7940.
(49) Yoshizawa, K.; Kagawa, Y.; Shiota, Y. *J. Phys. Chem. B* **2000**, *104*, 12365−12370.
(50) Ogliaro, F.; de Visser, S. P.; Cohen, S.; Sharma, P. K.; Shaik, S. *J. Am. Chem. Soc.* **2002**, *124*, 2806−2817.

the porphyrin without side chains because previous calculations of Cpd I of P450 showed negligible effects of alkyl porphyrin substituents on the state ordering and geometries.[18] Further test calculations which included the propionate side chains of protoporphyrin IX show that, as long as the propionates are screened by the positive arginines, there is no spin density on the propionates.

Supporting Information Available: Tables (13) with energies, group spin densities, charges, and geometric parameters are available. This material is available free of charge via the Internet at http://pubs.acs.org.

JA0380906